Available online at www.sciencedirect.com
ScienceDirect
Trans. Nonferrous Met. Soc. China 21(2011) 1917−1924
Transactions of Nonferrous Metals Society of China
www.tnmsc.cn

Effects of laser beam welding parameters on mechanical properties and microstructure of AZ31B magnesium alloy

G. PADMANABAN, V. BALASUBRAMANIAN

Center for Materials Joining & Research, Department of Manufacturing Engineering, Annamalai University, Annamalainagar 608 002, Tamil Nadu, India

Received 18 October 2010; accepted 31 December 2010

Abstract: The effects of laser beam welding process parameters such as laser power, welding speed and focal position on mechanical properties and microstructure of AZ31B magnesium alloy were studied. Nine joints were fabricated using different levels of laser power, welding speed and focal position. Tensile properties of the welded joints were evaluated and correlated with the weld zone microstructure and hardness. It is found that the joints fabricated using a laser power of 2 500 W, welding speed of 5.5 m/min and focal position of −1.5 mm yield superior tensile properties compared with the other joints. The formation of very fine grains in weld region, higher fusion zone hardness and uniformly distributed finer precipitates are the main reasons for superior tensile properties of these joints.

Key words: laser beam welding; magnesium alloy; tensile properties; laser power; welding speed; focal position

1 Introduction

Greater demand for reduced emissions and better fuel economy in passenger vehicles are the driving forces behind expanding the use of magnesium alloys. Environmental conservation is one of the principal reasons for the focus of attention on magnesium to provide vehicle mass reduction, CO_2 emission and fuel economy. Mass reduction through magnesium applications in the automotive industry is the effective option for decreasing fuel consumption and CO_2 emissions. The components that are made of magnesium alloys have better strength-to-density ratio, ductility and energy absorbing characteristics. Wrought alloys are currently used to a very limited extent, due to lack of suitable alloys and some technological restrictions imposed by the hexagonal crystal structure of magnesium. With the development of new grades of alloys, manufacturing techniques such as welding play an important role in exploiting the new fields of applications [1].

Gas tungsten arc welding (GTAW) and gas metal arc welding (GMAW) processes are the two important conventional fusion welding methods applied for joining magnesium alloys, especially for the removal and repair of casting defects. However, low welding speeds, large heat affected zone (HAZ) and fusion zone (FZ), high shrinkages, variations in microstructures and properties, evaporative loss of alloying elements, high residual stress and distortion of arc-welded joints have caused attention to be drawn towards laser beam welding (LBW). The advantages such as the low and precise heat input, small HAZ, deep and narrow FZ, low residual stress and weldment distortion, and high welding speed due to high power density, make the laser beam welding one of the best welding process to join magnesium alloys [2−6]. Crack-free laser welded joints with low porosity and good surface quality can be obtained for some magnesium alloys, in particular wrought material, using appropriate laser processing parameters [7].

Recently, some studies were carried out to evaluate the bead geometry and mechanical properties of laser beam welded magnesium alloys. MARYA et al [8] examined the weld morphology of laser beam welded AZ91 and AM50 magnesium alloy joints. For both alloys, important characteristics of the weld beads such as depth, width, crown height (hump), and surface ripples were analyzed as a function of the welding parameters, most particularly the heat input. ZHU et al [9] examined the defects formation during the diode and CO_2 laser beam welding of AZ31 magnesium alloy. They concluded that

Corresponding author: G. PADMANABAN; Tel: +91-4144-239734; Fax: +91-4144-238080/238275; E-mail: gknaban@rediffmail.com
DOI: 10.1016/S1003-6326(11)60950-3

diode laser welding produced significantly less porosity than the CO_2 laser welding. Microstructure and mechanical properties of laser beam welded AZ31B magnesium alloy were studied by COELHO et al [10]. They identified that the heat affected zone was very narrow, no grain coarsening was observed adjacent to the fusion line and microhardness values were almost uniform across base material HAZ and FZ. The effect of process parameters on the weld appearance and joint properties of laser beam welded AZ61 magnesium alloy was investigated by WANG et al [11]. They concluded that the refined grain structure was expected to contribute to the excellent mechanical properties of AZ61 weld beads. Most of the published papers have focused on analysing the weld bead formation in laser beam welding of magnesium alloy. Hence in this investigation, a systematic study was planned to evaluate the influence of welding parameters on mechanical and metallurgical properties of laser beam welded AZ31B magnesium alloy.

2 Experimental

The rolled plates of AZ31B magnesium alloy with 6 mm in thickness were cut into the required size (300 mm×150 mm) by machining process. Square butt joint configuration, as shown in Fig. 1, was prepared to fabricate the joints. The initial joint configuration was obtained by securing the plates in position using mechanical clamps. The direction of welding was normal to the rolling direction. Single pass welding procedure was used to fabricate the joints with the CO_2 laser welding machine (Make: Rofin slab; capacity: 6 kW). Argon gas was used as shielding gas with constant flow rate of 20 L/min. The chemical composition and mechanical properties of the base metal are presented in Tables 1 and 2, respectively. LBW process parameters used to fabricate the joints are presented in Table 3. The butt joints with high-quality can be obtained by the optimized processing. They are full penetration and lack of evident macroscopic porosities and inclusions in the fusion zone. The spot size and power density for various focal positions are presented in Table 4.

Figure 2 shows the optical microscope (OM) and scanning electron microscope (SEM) images of base metal. It basically contains coarse grains along with appreciable amount of sub-grains (Fig. 2(a)). From Fig. 2(b), grains with $Al_{12}Mg_{17}$ intermetallic compounds can be found. The $Al_{12}Mg_{17}$ intermetallic compounds are quite coarse and the distribution is non-uniform in the base metal.

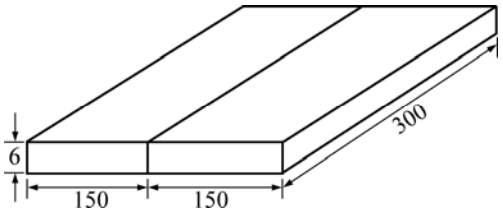

Fig. 1 Square butt joint configuration (Unit: mm)

Table 1 Chemical composition of base metal AZ31B magnesium alloy (mass fraction, %)

Al	Mn	Zn	Mg
3.0	0.20	1.0	Bal.

Table 2 Mechanical properties of base metal AZ31B magnesium alloy

Yield strength/MPa	Ultimate tensile strength/MPa	Elongation in gauge length of 50 mm/%	
171	215	14.7	
Reduction in cross -sectional area/%	Notch tensile strength/MPa	Notch strength ratio (NSR)	$HV_{0.49}$
14.3	192	0.89	69

Table 3 LBW process parameters used to fabricate joints

Joint number	Laser power/W	Welding speed/ ($m \cdot min^{-1}$)	Focal position/ mm	Heat input/ ($J \cdot mm^{-1}$)
1	2 500	5.0	−1.5	30
2	3 000	5.0	−1.5	36
3	3 500	5.0	−1.5	42
4	2 500	4.5	−1.5	33
5	2 500	5.0	−1.5	30
6	2 500	5.5	−1.5	27
7	2 500	5.0	0	30
8	2 500	5.0	−1.5	30
9	2 500	5.0	−3.0	30

Table 4 Spot size and power density for various focal positions

Joint number	Focal position/mm	Power/W	Spot size at work piece/mm	Power density/($W \cdot mm^{-2}$)	Spot size at exit of laser/mm	Focal length of lens/mm
1	0	2 500	0.180	98 244	24	300
2	−1.5	2 500	0.299	35 605	24	300
3	−3.0	2 500	0.418	18 218	24	300

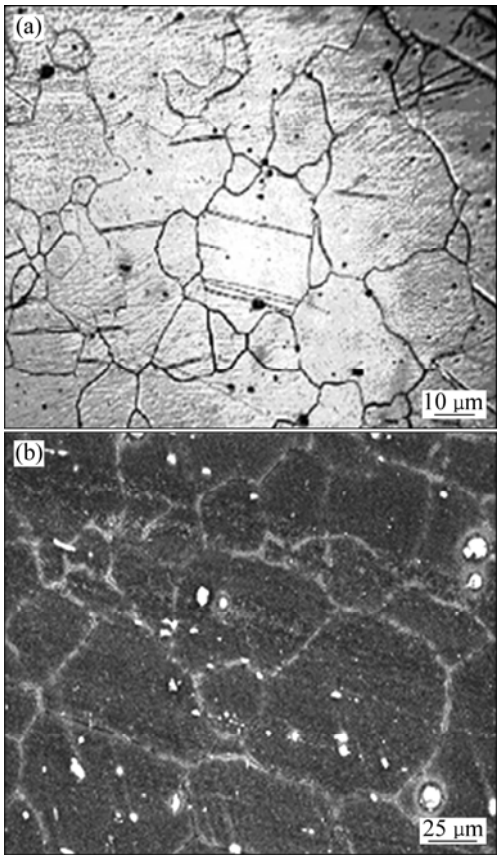

Fig. 2 OM (a) and SEM (b) micrographs of base metal

The welded joints were sliced and then machined to the required dimension, according to the ASTM E8M−04 standard for sheet type material (i.e., 50 mm gauge length and 12.5 mm gauge width). Two different tensile specimens were prepared to evaluate the transverse tensile properties of the welded joints. The smooth (unnotched) tensile specimens were prepared to evaluate yield strength, tensile strength and elongation of the joints. Notched specimens were prepared to evaluate notch tensile strength and notch strength ratio of the weld. Tensile test was carried out in 100 kN, electro-mechanical controlled universal testing machine (Make: FIE-Bluestar, India; Model: UNITEK−94100). The 0.2% offset yield strength was derived from the load—displacement diagram. The elongation was also evaluated and the values are presented in Tables 5−7. A Vickers microhardness testing machine (Make: SHIMADZU, Japan; Model: HMV−2T) was employed for measuring the hardness across the weld cross section with 0.49 N load for 20 s.

The specimens for metallographic examination were sectioned to the required size and then polished using different grades of emery papers. A standard reagent made of 4.2 g picric acid, 10 mL acetic acid, 10 mL diluted water and 70 mL ethanol was used to reveal the microstructure of the welded joints. Microstructural analysis was carried out using a light optical microscope

Table 5 Effect of laser power on transverse tensile properties of joints (welding speed=5.0 m/min; focal position=−1.5 mm)

Joint number	Laser power/W	Yield strength/ MPa	Ultimate tensile strength/MPa	Elongation in 50 mm gauge length/%	Reduction in cross-sectional area/%	Notch tensile strength/MPa	Notch strength ratio (NSR)	Joint efficiency/%
1	2 500	170	212	12.1	10.2	167	0.78	98.6
2	3 000	164	207	9.6	8.3	149	0.72	96.3
3	3 500	161	203	8.0	7.4	144	0.71	94.4

Table 6 Effect of welding speed on transverse tensile properties of joints (laser power=2 500 W; focal position=−1.5 mm)

Joint number	Welding speed/ ($m \cdot min^{-1}$)	Yield strength/ MPa	Ultimate tensile strength/MPa	Elongation in 50 mm gauge length/%	Reduction in cross-sectional area/%	Notch tensile strength/MPa	Notch strength ratio (NSR)	Joint efficiency/%
4	4.5	162	204	8.3	7.5	145	0.71	94.8
5	5.0	168	209	9.8	8.4	152	0.73	97.2
6	5.5	170	212	12.1	10.2	167	0.78	98.6

Table 7 Effect of focal position on transverse tensile properties of joints (laser power=2 500 W; welding speed=5.0 m/min)

Joint number	Focal position/ mm	Yield strength/ MPa	Ultimate tensile strength/MPa	Elongation in 50 mm gauge length/%	Reduction in cross-sectional area/%	Notch tensile strength/MPa	Notch strength ratio (NSR)	Joint efficiency/%
7	0	154	193	8.2	7.1	136	0.70	89.7
8	−1.5	170	212	12.1	10.2	167	0.78	98.6
9	−3.0	152	190	7.9	7.0	129	0.67	88.4

(OM) (Make: MEIJI, Japan; Model: MIL−7100) incorporated with an image analyzing software (Metal Vision), a scanning electron microscope (SEM) (Make: JOEL, Japan; Model: 5610 LV) and a transmission electron microscope (TEM) (Make: Philips, UK; Model: CM20). EDAX analysis was carried out using TEM at high magnification to estimate the mass fraction of elements (Make: Philips, UK: Model: CM20).

3 Results

3.1 Tensile properties

The transverse tensile properties such as yield strength, tensile strength, elongation, reduction in cross-sectional area, notch tensile strength, notch strength ratio and joint efficiency of laser beam welded AZ31B magnesium alloy joints were evaluated. In each condition, three specimens were tested and the average of three results is presented in Tables 5−7. Of the nine joints fabricated, the joint fabricated with a laser power of 2 500 W, welding speed of 5.5 m/min and focal position of −1.5 mm exhibited higher yield strength (170 MPa), tensile strength (212 MPa), elongation (12.1%) and reduction in cross sectional area (10.2%).

Notch strength ratio (NSR) is the ratio between the tensile strength of notched specimen at maximum load to the ultimate tensile strength of unnotched specimen. NSR is found to be less than unity (<1) for all the joints. This suggests that the AZ31B magnesium alloy is sensitive to notches and falls in to the 'notch brittle materials' category. The NSR is 0.89 for the unwelded parent metal and LBW causes reduction in NSR of the weld metal. The joint fabricated with a laser power of 2 500 W, welding speed of 5.5 m/min and focal position of −1.5 mm exhibited higher notch strength ratio (0.78), which is 12% lower compared with that of the unwelded parent metal. Joint efficiency is a ratio between the tensile strength of welded joint and the tensile strength of unwelded parent metal. The joint fabricated with a laser power of 2 500 W, welding speed of 5.5 m/min and focal position of −1.5 mm exhibited a maximum joint efficiency of 98.6%.

3.2 Microhardness

The hardness was measured along the mid-thickness line of the cross-section of the joint using Vickers microhardness testing machine and the values are presented in Fig. 3. The hardness of base metal (unwelded parent metal) is HV 69. The joint fabricated with a laser power of 2 500 W, welding speed of 5.5 m/min and focal position of −1.5 mm recorded higher hardness (HV 76) in the weld region, and this is also one of the reasons for superior tensile properties of these joints compared with the other joints. The location of failure in all the tensile specimens was invariably at the transition region (Fig. 4), which is consistent with the lowest hardness distribution in the transition region (Fig. 3).

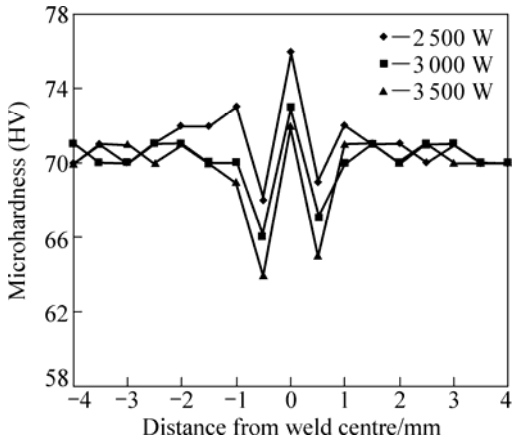

Fig. 3 Microhardness plots of joint with different laser powers

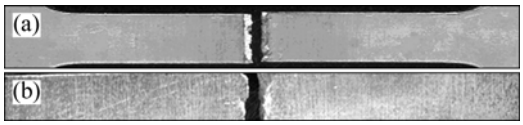

Fig. 4 Failure location of LBW joint during tensile test: (a) Top view; (b) Cross sectional view

3.3 Microstructure

The microstructures of fusion zone of all the joints are displayed in Figs. 5−7. From the micrographs, it is understood that the LBW parameters have appreciable influence on the average grain diameter of weld region in AZ31B magnesium alloy. Compared with the base metal, the microstructures in the center of the fusion zone of all the joints are more homogeneous and characteristic of numerous equiaxed grains. This can be due to the grain refining effect of the Al addition and rapid solidification [12]. Of the nine joints fabricated, the joints fabricated with a laser power of 2 500 W, welding speed of 5.5 m/min and focal position of −1.5 mm contain finer equiaxed grains in the weld region compared with the other joints. Furthermore, a large number of precipitated particles are observed evidently in the weld region and the concentration of precipitates is moderate. This is also one of the reasons for higher tensile properties of these joints compared with the other joints.

To identify the reason for failure in transition region, the detailed microstructural analysis was carried out across the joint using scanning electron microscope (Fig. 8). From the SEM images, it is inferred that there is an appreciable variation in grain size across the weld. The fusion zone contains finer grains with finer $Al_{12}Mg_{17}$ intermetallic compounds which are homogeneously distributed in the magnesium matrix (Fig. 8(c)). The

SEM image of transition region is shown in Fig. 8(d). The sharp transition from the base metal to the weld region indicates that there is no HAZ and similar observation was made by other investigators also [13−14]. Appreciable variation in hardness at the fusion boundaries was observed (Fig. 3). Though heat-affected zone was not observed under microscope, it may be present at the fusion boundaries and that may be one of the reasons for variation in hardness at fusion boundaries. At the outset, the annealing softening in these regions might have decreased the hardness [15]. This may be another reason for failure along the transition region.

TEM micrograph of fusion zone of LBW joint is shown in Fig. 8(e). From the TEM micrograph, it is found that the fusion zone of LBW joint contains finer magnesium grains with finer $Al_{12}Mg_{17}$ precipitates as compared with base metal. The distributions of $Al_{12}Mg_{17}$ precipitates are uniform throughout the magnesium matrix as compared with base metal. The XRD results presented in Fig. 8(f) confirm the presence of $Al_{12}Mg_{17}$ precipitates in fusion zone along with the traces of Mg_2Zn_{11}. The EDAX results are also presented in Fig. 9 to determine the composition of precipitates.

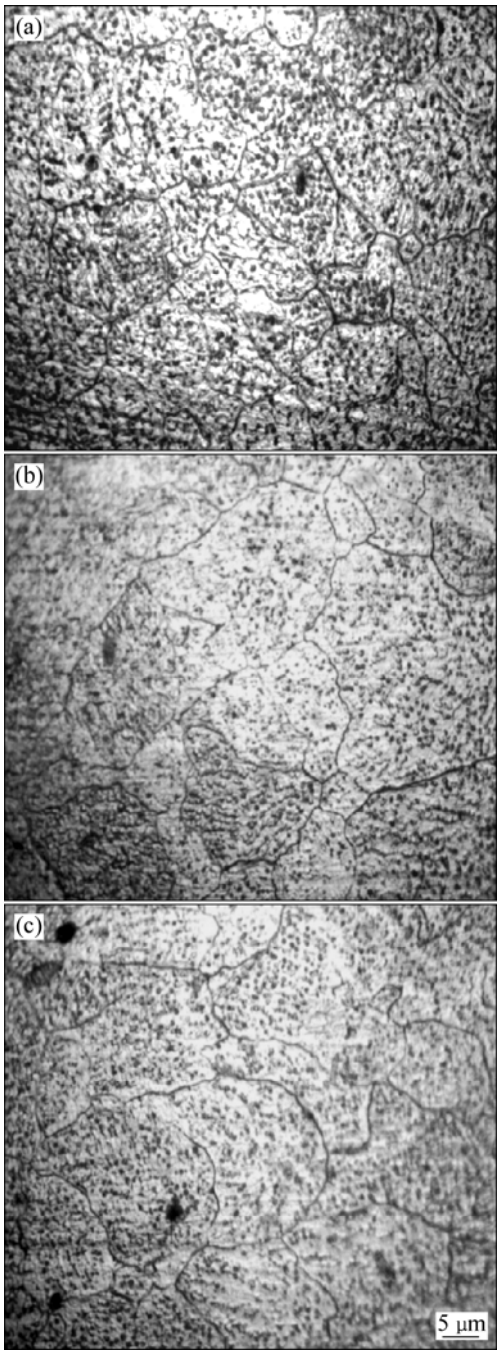

Fig. 5 Microstructures of fusion zone with different laser powers: (a) 2 500 W; (b) 3 000 W; (c) 3 500 W

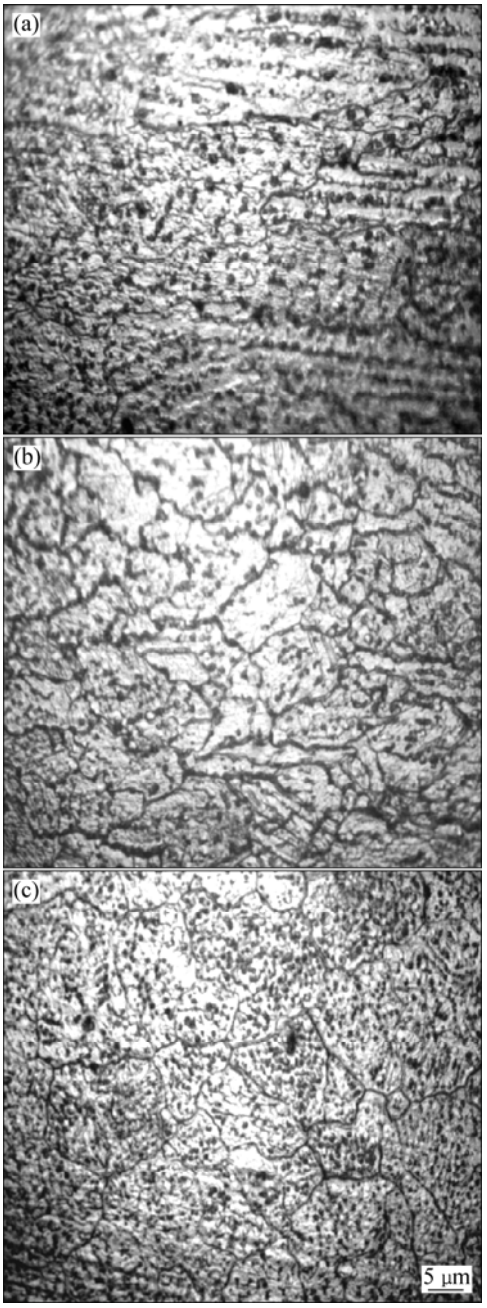

Fig. 6 Microstructures of fusion zone with different welding speeds: (a) 4.5 m/min; (b) 5.0 m/min; (c) 5.5 m/min

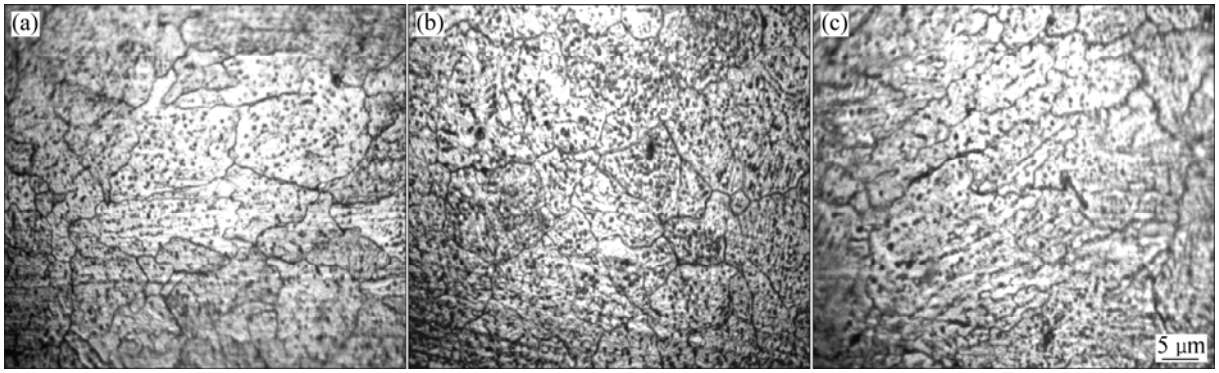

Fig.7 Microstructures of fusion zone with different focals positions: (a) 0 mm; (b) −1.5 mm; (c) −3.0 mm

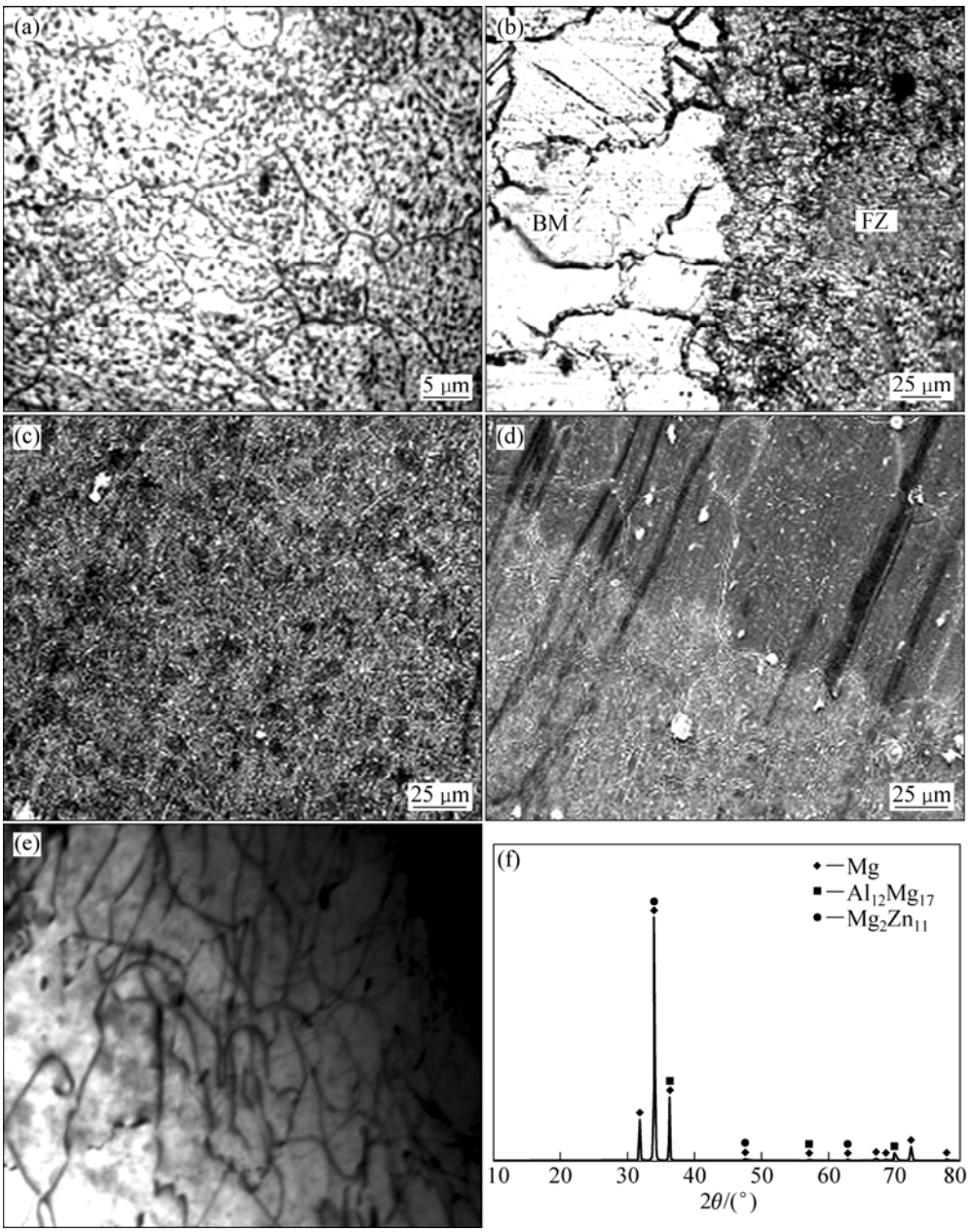

Fig. 8 Microstructural features of joint exhibiting superior tensile properties: (a) Fusion zone (OM); (b) Transition zone (OM); (c) Fusion zone (SEM); (d) Transition zone (SEM); (e) Fusion zone (TEM); (f) XRD pattern

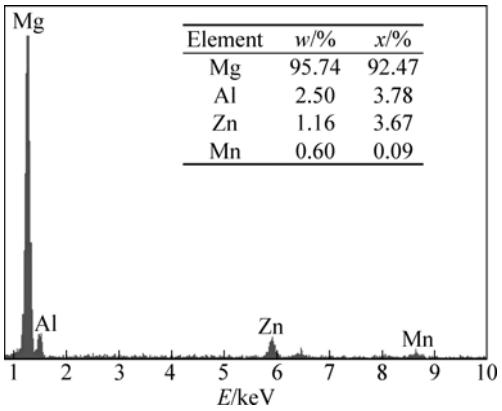

Element	w/%	x/%
Mg	95.74	92.47
Al	2.50	3.78
Zn	1.16	3.67
Mn	0.60	0.09

Fig. 9 EDAX analysis of joint

4 Discussion

The heat input is directly related to the laser power and welding speed, i.e., the heat input can be controlled with the change of the laser power or welding speed. From the tensile test results, it could be inferred that the joints fabricated with a laser power of 2 500 W, welding speed of 5.5 m/min and focal position of −1.5 mm exhibit superior tensile properties compared with the other joints. This is mainly because relatively lower heat input leads to the formation of finer grains and finer precipitates. The increase in laser power leads to an increase in the heat input. The grains in fusion zone get coarser while increasing the heat input (Fig. 5(c)). This phenomenon can also be explained by the change of cooling rate. It is known that an increase in heat input will result in slow cooling rate. Moreover, the slower the cooling rate during solidification, the longer the time available for grain coarsening. In contrast, the decrease in laser power leads to decrease in heat input. This leads to faster the cooling rate and subsequently finer the grain size of fusion zone [16]. It can also be noted that the precipitate concentration in the fusion zone is more, as the heat input is increased. This is mainly due to the decreased cooling rate with increasing heat input. QUAN et al [17] reported that during the laser welding process, the melt alloy was quickly solidified and cooled to room temperature, and the maximum solid solubility of Al decreased immediately from 12.7% to about 2.0% (mass fraction). The remnant Al was precipitated as γ-$Mg_{17}Al_{12}$ phase. The more concentration of precipitates deteriorated the tensile properties of the joints. In contrast, with decreasing the heat input, the cooling rate increased, so most Al atoms could not return to the grain boundary in time, and the concentration of precipitates was moderate (Fig. 5(a)).

The welding speed is always in inverse proportion with heat input. An increase in welding speed leads to a decrease in heat input. The microstructure of the laser welds is a high-speed process in which heat is rapidly extracted from the molten fusion zone by the surrounding base material. So, the grain growth can be minimized at high welding speeds, and the finer grains are obtained in the fusion zone [18]. In contrast, as the welding speed decreases, the heat input increases subsequently. Lower welding speed results in higher heat input and slow cooling rate leads to grain coarsening. It can also be noted that the precipitate concentration in the fusion zone is more, as the welding speed is decreased (Fig. 6(a)). The concentration of precipitates is moderate, as the welding speed is increased (Fig. 6(c)).

Using a focused beam results in the increase of the power density, which means the heat will localize in small metal portion. The position that gave the maximum power density was deemed the focal position. When the focal position was 0 mm, higher power density or longer interaction time was obtained. This promoted the grain growth in the fusion zone (Fig. 7(a)). When the focal position was −1.5 mm, the optimum weld was obtained. The optimum power density (35 605 W/mm^2) might have reduced the grain size (Fig. 7(b)) which resulted in the increase of tensile strength. The optimum power density was characterized by the formation of finer precipitates in the fusion zone.

5 Conclusions

1) The joint fabricated with the laser power of 2 500 W, welding speed of 5.5 m/min and focal position of −1.5 mm shows higher tensile properties compared with their counterparts.

2) The formation of very fine grains in weld region, higher fusion zone hardness and uniformly distributed finer precipitates are the main reasons for superior tensile properties of the joint.

Acknowledgements

The authors are grateful to the Department of Manufacturing Engineering, Annamalai University, Annamalai Nagar, India for extending the facilities of Material Testing Laboratory to carryout this investigation. The authors are also grateful to Centre for Laser Processing of Materials (CLPM), ARCI, Hyderabad to carry out the laser experiments. The authors wish to place their sincere thanks to Science and Engineering Research Council (SERC), Department of Science and Technology (DST), New Delhi for financial support rendered through a R&D project No. SR/S3/MERC-062/2004.

References

[1] KULEKCI M K. Magnesium and its alloys applications in automotive industry [J]. Int J Adv Manu Tech, 2008, 39(9−10): 851-−865.

[2] HAFERKAMP H, BACH F W, BURMESTER I, KREUTZBURG K, NIEMEYER M. Nd:YAG laser beam welding of magnesium constructions [C]//Proceedings of the Third International Magnesium Conference (UMIST). Manchester, UK, 1996: 89−98.

[3] MARYA M, EDWARDS G, MARYA S, OLSON D L. [C]// Proceedings of the Seventh JWS International Symposium. Kobe, 2001: 597−602.

[4] HAFERKAMP H, NIEMEYER U DILTHEY, TRAGER G. Weld Cutt, 2000, 52(8): 178−180.

[5] HAFERKAMP H U, DILTHEY M, TRAGER G, BURMESTER I, NIEMEYER M. Beam welding of magnesium alloys [C]//Proceedings Conference: Magnesium Alloys and their Applications. Wolfsburg, Germany, 1998: 595−600.

[6] HAFERKAMP H, von ALVENSLEBEN M, GOEDE M, NIEMEYER J, BUNTE. Fatigue strength of laser beam welded magnesium alloys [C]//Proceeding of the 32nd International Symposium on Automotive Technology and Automation (ISATA) on Advances in Automotive and Transportation Technology and Practice for the 21st Century. Vienna, Austria, 1999: 389−397.

[7] CAO X, JAHAZI M, IMMARIGEON J P, WALLACE W. A review of laser welding techniques for magnesium alloys [J]. J Mater Process Tech, 2006, 171: 188−204.

[8] MARYA M, EDWARDS G R. Factors controlling the magnesium weld morphology in deep penetration welding by a CO_2 laser [J]. J Mater Eng Perform, 2000, 10: 435.

[9] ZHU Jin-hong, LI Lin, LIU Zhu. CO_2 and diode laser welding of AZ31 magnesium alloy [J]. Appl Sur Sci, 2005, 247: 300−311.

[10] COELHO R S, KOSTKA A H, PINTO, RIEKEHR S, KOÇAK M, PYZALLA A R. Microstructure and mechanical properties of magnesium alloy AZ31B laser beam welds [J]. Mater Sci Eng A, 2008, 485(1−2): 20−30.

[11] WANG H Y, LI Z J. Investigation of laser beam welding process of AZ61 magnesium based alloy [J]. Acta Metall Sin (Eng Lett), 2006, 19: 287−294.

[12] LIU Li-ming, WANG Ji-feng, SONG Gang. Hybrid laser—TIG welding, laser beam welding and gas tungsten arc welding of AZ31B magnesium alloy [J]. Mater Sci Eng A, 2004, 381: 129−133.

[13] KANNAN M B, DIETZEL W, BLAWERT C, RIEKEHR S, KOCAK M. Stress corrosion cracking behavior of Nd:YAG laser butt welded AZ31 Mg sheet [J]. Mater Sci Eng A, 2007, 444: 220−226.

[14] YU Z H, YAN H G, GONG X S, QUAN Y J, CHEN J H, CHEN Q. Microstructure and mechanical properties of laser welded wrought ZK21 magnesium alloy [J]. Mater Sci Eng A, 2009, 523: 220−229.

[15] KOLODZIEJCZAK P, KALITA W. Properties of CO_2 laser-welded butt joints of dissimilar magnesium alloys [J]. J Mater Process Tech, 2009, 209: 1122−1128.

[16] KOU S. Welding metallurgy [M]. 2nd ed. New Jersey: John Wiley & Sons, 2003: 460.

[17] QUAN Y J, CHEN Z H, GONG X S, YU Z H. Effects of heat input on microstructure and tensile properties of laser welded magnesium alloy AZ31 [J]. Mater Charac, 2008, 59(10): 1491−1497.

[18] QUAN Y J, CHEN Z H, GONG X S, YU Z H. CO_2 laser beam welding of dissimilar magnesium-based alloys [J]. Mater Sci Eng A, 2008, 496: 45−51.

激光束焊接参数对 AZ31B 镁合金力学性能和显微组织的影响

G. PADMANABAN, V. BALASUBRAMANIAN

Center for Materials Joining & Research, Department of Manufacturing Engineering,
Annamalai University, Annamalainagar 608 002. Tamil Nadu, India

摘　要：研究激光束焊接工艺参数如激光功率、焊接速度和焦点位置对 AZ31B 镁合金力学性能和显微组织的影响。采用不同的激光功率、焊接速度和焦点位置焊接了 9 种接头。焊接接头的拉伸性能与焊接区的微观组织和硬度有关。结果表明，采用激光功率 2 500W，焊接速度 5 m/min，焦点位置−1.5 mm 时，所得的接头具有优良的拉伸性能。焊接区细晶粒的形成、较高的融化区硬度、均匀分布的细小析出物是得到优良拉伸性能的主要原因。

关键词：激光束焊接；镁合金；拉伸性能；激光功率；焊接速度；焦点位置

(Edited by LI Xiang-qun)